Biochimica et Biophysica Acta 1820 (2012) 469–481

Contents lists available at SciVerse ScienceDirect

Biochimica et Biophysica Acta

journal homepage: www.elsevier.com/locate/bbagen

# Differential role of actin-binding proteins in controlling the adipogenic differentiation of human CD105-positive Wharton's Jelly cells ☆

Kang-Wei Peng [a], Ying-Ming Liou [a,b,*]

[a] Department of Life Sciences, National Chung-Hsing University, Taichung 402, Taiwan
[b] Graduate Institute of Basic Medical Science, China Medical University, Taichung 40402, Taiwan

ARTICLE INFO

*Article history:*
Received 27 September 2011
Received in revised form 30 December 2011
Accepted 24 January 2012
Available online 8 February 2012

*Keywords:*
WJCs
ABPs
Small interfering RNAs
Overexpression
Atomic force microscopy

ABSTRACT

*Background:* Wharton's Jelly cells (WJCs) can be differentiated into adipocytes by cytoskeletal reorganisation in association with changes in the mechanical properties of cells.
*Methods:* WJCs subjected to adipocyte induction were observed changes in the cell morphology and alterations in actin filament formation. Transfection with either small interfering RNAs (siRNAs) against formin-2 (FMN-2), tropomyosin-1 (Tm-1), caldesmon (CaD), and profilin (Pro) or a pcDNA6-gelsolin (GSN)-constructed vector in WJCs was used to establish their regulatory roles in controlling adipogenesis. Phenotypic transformation of the cell shape and changes in cell surface adhesion force were determined in WJCs after transformation.
*Results:* The levels of protein and mRNA expression of β-actin and several key actin binding ptoteins (ABPs) were decreased during the early stage of adipogenic induction but were recovered in the later induction. The siFMN-2, siTm-1, siCaD, and siPro gene knockdown in WJCs caused a widening of the cell shape, while WJCs overexpressing GSN retained a fibroblast cell shape. For both transformations, atomic force microscopy revealed alterations in the biomechanical signals on the cell surface. However, the adipogenic potency was increased after siFMN-2, siTm-1, siCaD, and siPro gene knockdown and decreased during GSN overexpression.
*Conclusions:* siRNA gene knockdown of siFMN-2, siTm-1, siCaD, and siPro enhances the potency for WJCs commitment to adipocyte, while GSN overexpression modulates the PPAR-γ-independent pathway for the adipogenesis of WJCs.
*General significance:* The phenotypic changes associated with decreased ABP gene expression are critical for regulating the adipogenic differentiation of WJCs through the temporal control of actin filament organisation.


## 1. Introduction

Wharton's Jelly cells (WJCs) extracted from human umbilical cords possess the capacity of self-renewal and differentiation into multiple cell types, including mature adipocytes, osteoblasts, chondrocytes, skeletal myocytes, cardiomyocytes, neurons, and endothelial cells [1–5]. In addition, WJCs possess immune properties that would be permissive to allogeneic transplantation [2]. WJCs could be isolated by different methods with or without enzymatic dissociation processes. A recent study focused on the efficiency of the isolation procedure and expansion of cells from WJCs isolated from human umbilical cords without enzyme digestion or dissection [6]. This procedure established a simple, rapid, and reproducible protocol to isolate abundant WJCs from short segments of umbilical cords.

WJCs have been successfully differentiated into adipocytes [1–5]. During the process of differentiation, the committed cells exhibit a number of phenotypic changes, including biochemical, structural, and transcriptional reorganisation. Adipogenic differentiation is initiated by several transcription factors, such as the peroxisome proliferator activated receptor (PPAR)-γ2 [7]. Cellular transformation is accomplished by expressing structural proteins involved in cytoskeletal remodelling [8] and lipid granule-specific surface proteins, such as adipophilin [9], followed by the expression of specific enzymes, such as fatty acid synthase (FAS) [5]. The final step in adipogenic

*Abbreviations:* WJCs, Wharton's Jelly cells; ABPs, actin-binding proteins; FMN-2, formin-2; Tm, tropomyosin; GSN, gelsolin; siRNAs, small interfering RNAs; CaD, caldesmon; siCaD, siRNA against CaD; PPAR-γ2, peroxisome proliferator activated receptor; FAS, fatty acid synthase; FBS, foetal bovine serum; qPCR, quantitative reverse transcription polymerisation chain reaction; PBS, phosphate buffer saline; Fura 2-AM, fura 2-tetra-acetoxymethyl ester; RP, rhodamine phalloidin; AFM, atomic force microscopy; GSN op, GSN overexpression; siGSN, siRNA against GSN; HUCSCs, human umbilical cord stromal cells

☆ The authors declare no potential conflicts of interest.

* Corresponding author at: National Chung-Hsing University, 250 Kuokang Road, Taichung 402, Taiwan. Tel.: +886 4 22851802; fax: +886 4 22851802.
*E-mail address:* ymlion@dragon.nchu.edu.tw (Y.-M. Liou).

0304-4165/$ – see front matter © 2012 Elsevier B.V. All rights reserved.
doi:10.1016/j.bbagen.2012.01.014

differentiation is the establishment of endocrine function characterised by the production of the adipocyte-specific hormone, leptin, which is elevated during terminal adipogenic differentiation [10].

Increasing evidence shows that continuous actin filament remodelling via a multitude of actin-binding proteins (ABPs) is closely related to adipogenic differentiation in mesenchymal stem cells (MSCs) [11–14]. However, the regulatory mechanisms of the actin-based processes that govern cell shape changes and adipogenic differentiation remain unknown. Formin, a processive motor, together with profilin (Pro) can nucleate the polymerisation of straight actin filaments associated with ATP hydrolysis [15]. Formin-2 (FMN-2) is a formin homolog, and its expression has been reported only in the brain and spinal cord [16] and oocytes [17]. Recently, we showed that FMN-2 is expressed in human umbilical WJCs and plays a role in intracellular $Ca^{2+}$ signalling during the proliferation of CD105-positive WJCs [18]. Gelsolin (GSN) is one of the actin filament-severing proteins that play a key role in the regulation of actin filament assembly and disassembly [19]. Tropomyosin (Tm) is a coiled-coil protein that stabilises actin filaments by modulating their interaction with other actin-associated proteins in cells [20]. A large family of more than 40 Tm isoforms is derived from four highly conserved genes, Tm-1, Tm-2, Tm-3, and Tm-4, via multiple promoters and alternative splicing, and these isoforms are associated with different specialised actin microfilament ensembles in cells [21,22]. Caldesmon (CaD) is a protein that binds to $Ca^{2+}$/calmodulin, Tm, actin, and myosin in cells [23]. Two isoforms of CaD are produced from a single gene [24] through alternative splicing: the smooth muscle form h-CaD, with a high molecular weight of 130–140 kDa [25], and the non-muscle l-CaD, with a low molecular weight of 60–90 kDa [26]. Recent studies suggest that l-CaD plays a role in the regulation of cytoskeleton organisation by modulating the contractility and stabilisation of the stress fibres [27].

In this study, we used human CD105-positive WJCs to examine whether adipogenic-induced phenotypic changes are associated with alterations in the expression of ABPs in WJCs. Adipogenesis was determined by oil red O staining and by the increased expression of key adipogenic markers, including PPAR-γ2, adipophilin, FAS, and leptin. To establish the regulatory roles of ABPs in governing adipogenic differentiation, WJCs were transfected with either small interfering RNAs (siRNAs) against FMN-2, Pro, CaD, and Tm-1 or a pcDNA6-GSN-constructed vector. The siFMN-2, siPro, siCaD, and siTm-1 gene knockdown in WJCs resulted in a phenotypic transformation of the cell shape to a "broader" form. In contrast, WJCs overexpressing GSN retained a fibroblast cell shape. For both transformations, WJCs showed elevated cell surface adhesion as measured by atomic force microscopy. However, the adipogenic potency was increased after siFMN-2, siPro, siCaD, and siTm-1 gene knockdown and decreased after GSN overexpression. Thus, the decreased ABP gene expression in the early stages of adipogenesis might act to modulate the actin filament organisation to influence subsequent events for the adipogenic differentiation of WJCs.

## 2. Materials and methods

### 2.1. Culture of CD105-positive WJCs from human umbilical cords

Protocols for sampling human umbilical cord were approved by the Institutional Review Board of China Medical University Hospital (DMR97_IRB-169). Human umbilical cords were obtained aseptically and washed with phosphate buffered saline (PBS) containing 1% streptomycin (100 μg/ml) (Gibco, Invitrogen Taiwan Ltd., Taipei, Taiwan) and 1% penicillin (100 U/ml) (Gibco). Wharton jelly tissues separated from the vessels and amniotic membranes were then transferred to a sterile container in 1% antibiotics containing PBS. The tissues were scraped off from the Wharton's jelly with a scalpel and centrifuged at 250×*g* for 5 min at room temperature. The pellet was washed with 1% antibiotics containing PBS, and then treated with 2 mg/ml collagenase I (Sigma, St Louis, MO) at 37 °C for 2 h, followed by washing with 1% antibiotics containing Dulbecco's modified essential medium (DMEM) (Gibco), and finally digesting with 0.5 ml TrypLE (Gibco) at 37 °C for 10 min. After removal of TrypLE, the tissues were grown in a 6-cm dish with 10% foetal bovine serum (FBS) (Gibco)-DMEM DMEM containing 4.5 g/l glucose under 5% $CO_2$ atmosphere in a 37 °C incubator. After several passages the dispersed cells were used to further isolate the cell population expressing a cell surface marker CD105 by using a commercially available magnetic absorption cell sorting (MACS) kits (Miltenyi Biotec Inc., Auburn, CA) according to the procedures recommended by the manufacturer. The CD105-positive cells were then used directly for cultures or stored in liquid nitrogen for later use.

### 2.2. Adipogenic differentiation

Subconfluent (90%) CD105-positive WJCs cultured on glass coverslips in 6-well plates were treated with the adipogenic medium containing 1 μM dexamethasone (Sigma), 0.5 μM 3-isobutyl-1-methylxanthine (Sigma), 200 μM indomethacin (Sigma), 10 μM insulin (Gibco), 100 units/ml penicillin (Gibco), 100 μg/ml streptomycin (Gibco), 10% FBS (Gibco), and 4.5 g/l of glucose in DMEM (Gibco). Medium was replaced every 3 days for a 4-week period. On days 0 (control), 1, 4, 7, 14, and 21, the cells were fixed in 10% buffered formalin (Sigma) for 10–20 min at room temperature and stained with 10% (wt/vol) oil red O (Sigma) for 10 min. Haematoxylin (Sigma) was used as a nuclear counterstain.

In addition, adipogenesis was determined by the increased mRNA expression of key adipogenic markers, including peroxisome proliferator activated receptor (PPAR)-γ2, adipophilin, fatty acid synthase (FAS), and leptin. The procedures for RNA extraction [18] and real-time quantitative reverse transcription polymerisation chain reaction (qPCR) are described in the Supplementary data.

### 2.3. Immunocytochemistry, fluorescence staining and laser-scanning confocal microscopy

CD105-positive WJCs (2 $10^4$) were seeded on a glass coverslip in each well of a 12-well plate and cultured in DMEM-10% FBS for 24 h in a $CO_2$ incubator at 37 °C; after this time period, the medium was replaced with adipogenic medium. On days 0, 1, 4, 7, 14, or 21, the cells were fixed in 4% paraformaldehyde (Sigma) for 15 min, permeabilised with 0.1% Triton X-100 (Sigma) for 1 min, blocked with 2% bovine serum albumin (Sigma) for 30 min (all at room temperature), and then incubated with primary antibodies in PBS as described in the Supplementary data.

### 2.4. Immunoblotting

The cells were lysed with pre-chilled RIPA buffer containing 50 mM Tris–HCl, pH 7.4, 150 mM NaCl, 1% Nonidet P-40, 0.25% sodium deoxycholate, 5 mM EDTA, 0.02 mM EGTA, 1% phenylmethanesulfonyl fluoride, and a cocktail of protease inhibitors (Sigma). After centrifugation, the pellet was washed with RIPA buffer followed by Tris buffer (50 mM, pH 8.0). The procedures for immunoblotting are described in the Supplementary data.

### 2.5. Semi-quantitative RT-PCR and real-time qPCR for quantification of mRNA expression of actin and actin-binding proteins

CD105-positive cells ($10^7$) were seeded in a 10-cm dish in DMEM-10% FBS and cultured in a $CO_2$ incubator at 37 °C for 24 h. Subsequently, the cells were changed to fresh adipogenic medium for 0, 1, 4, 7, 14, or 21 days. The procedures for RNA extraction, semi-quantitative reverse

transcription polymerisation chain reaction (semi-quantitative RT-PCR), and qPCR are described in the Supplementary data.

### 2.6. Silencing of CaD expression by small interfering RNAs (siRNAs)

Sixty to eighty percent confluent cells were transfected with either the scrambled control siRNAs (sc-36869) or siRNAs directed to human CaD (sc-35768) according to the manufacturer's guidelines (Santa Cruz Biotechnology, Santa Cruz, CA). The cells received 10 μM siRNA and were incubated for 6 h at 37 °C in a $CO_2$ incubator. At 24 or 48 h after transfection, total RNA was extracted for reverse transcription and qPCR measurements to confirm the downregulation of CaD expression. After siRNA exposure for 48 h, western blot analysis was performed to verify the attenuation of protein content.

### 2.7. Atomic force microscopy

DI-Dimension 3100 AFM (Digital Instruments, Santa Barbara, CA) was applied to obtain cell surface contour images in contact mode and measure the interfacial forces in tapping mode [28]. The V-shaped silicon cantilevers with a spring constant of ~0.9–0.12 N/m were used for imaging cell surface areas (20×20 μm) in phosphate buffer. Approximately 10–20 spots of this scanning region were randomly selected using the same probe to extend forward 1 nm deep and to retract back to the starting point. The retracting force–distance curves were used to calculate the adhesion forces that correspond to the elasticity of cell membrane surface.

### 2.8. GSN overexpression

The pc6-GSN plasmid construct was cotransfected with GSN into CD105-positive WJCs using lipofectamine 2000 (Invitrogen). The full-length cytoplasmic GSN cDNA [29] was cloned into the expression vector pcDNA6-V5/His. Before transfection, the CD105-positive WJCs were cultured in a 6-well plate containing culture medium without antibiotics at a density of 70–80% confluence. Both the lipofectamine and DNA constructs were diluted with transfection medium without serum and incubated for 5 min. Subsequently, the diluted DNA constructs and diluted lipofectamine were mixed at a 1:2.5 ratio of DNA to lipofectamine. After gentle shaking and incubation for 20 min, the DNA-lipofectamine complexes were added to each well and incubated in a $CO_2$ incubator at 37 °C for 6 h. The culture medium was replaced with serum-containing DMEM.

### 2.9. Intracellular $Ca^{2+}$ measurements in cellular suspensions

Fura 2-AM (fura 2-tetra-acetoxymethyl ester) (Molecular Probes, Eugene, OR) was used as a fluorescence indicator. The procedures for fura 2-AM loading in cells and intracellular $Ca^{2+}$ measurements were described previously [18].

### 2.10. Statistics

Quantitative values are expressed as the mean ± SEM. Comparisons were performed using Student's *t* test; P values less than 0.05 were considered significant.

## 3. Results

### 3.1. The involvement of cytoskeletal reorganisation in the adipogenic differentiation of WJCs

As previously reported [4,5], WJCs isolated from human umbilical cords displayed a fibroblast-like phenotype and expressed high levels of matrix markers (CD44, CD105), integrin markers (CD29, CD51), and MSC markers (SH2, SH3) but did not express hematopoietic lineage markers (CD34, CD45). These cells have been successfully induced differentiation into mature adipocytes, osteoblasts, chondrocytes, cardiomyocytes, and neurons [4,5]. In addition, we isolated CD105-positive MSCs from human umbilical WJCs for defining the roles of actin-binding proteins (ABPs) in the regulation of actin filament assembly associated with cellular signal transduction pathways in stromal cell proliferation [18]. In the present study, human CD105-positive WJCs were used to examine whether adipogenic-induced phenotypic changes are associated with alterations in the expression of ABPs in WJCs.

During adipogenic induction, WJCs underwent cell transformations, including cell shape changes (Fig. 1A), cytoplasmic lipid droplet accumulations (Fig. 1B), and cytoskeletal reorganisation (Fig. 1D). The oil red O staining assay revealed that cytoplasmic lipid droplets were accumulated in WJCs at 4 days post-induction and levelled off after 14 days (Fig. 1B). In addition, adipogenesis was confirmed by the expression of the adipogenic transcription factor, PPAR-γ2 (Fig. 1C, top panel), and other adipocyte-related marker proteins, including adipophilin, FAS, and leptin (Fig. 1C, bottom panel). The mRNA expression of PPAR-γ2 and adipophilin, which is required during the early events of adipogenesis [7–9], was increased in WJCs at 4 days post-induction and peaked after 14 or 21 days (Fig. 1C). In contrast, the mRNA expression levels of FAS and leptin, which are hallmarks of terminal adipogenic differentiation, were not significantly changed in WJCs at 4 days post-induction but markedly increased after 14 or 21 days (bottom panel in Fig. 1C).

Confocal fluorescence microscopy revealed that the formation of rhodamine phalloidin (RP)-labelled F-actin was decreased in WJCs at 1 day post-induction but gradually recovered after 7 days (Fig. 1D), suggesting that a decrease in F-actin formation occurs early during the adipogenic differentiation of WJCs. CaD is known to modulate the stabilisation of stress fibres in WJCs [18]. Thus, the visual observation of colocalisation between CaD and RP-labelled F-actin by fluorescence microscopy could demonstrate the association of F-actin with stress fibres in WJCs during adipogenic induction. The colocalisation of CaD with RP-labelled F-actin was significantly decreased at 7 or 14 days post-induction (Fig. 1E, top-row panels), suggesting that the F-actin associated stress fibres were attenuated during terminal adipogenic differentiation. In addition, immunocytochemistry of the tubulin-based cytoskeleton (bottom row in Fig. 1E) showed that adipocyte induction also resulted in remodelling of the microtubule cytoskeleton concomitant with changes in the cell shape. Phase contrast micrographs showing lipid droplets associated with the microtubule cytoskeleton also suggested that microtubule cytoskeletal reorganisation is associated with the adipogenic induction of WJCs (right bottom corner in Fig. 1E). Collectively, these results demonstrate that cytoskeletal remodelling is involved in governing the morphological changes in WJCs during adipogenic induction.

### 3.2. The involvement of ABPs in the induction of the adipogenic differentiation of WJCs

Western blot analyses indicated that after 1 or 4 days of adipogenic induction, the β-actin protein level was decreased by 60% or 90%, respectively, and returned to the control levels after 14 or 21 days (left panel in Fig. 2A). Real-time quantitative PCR (qPCR) measurements revealed that β-actin mRNA was decreased by 14%, 60%, 70%, and 70% in WJCs after induction for 1, 4, 14, or 21 days, respectively (right panel in Fig. 2A). This result is consistent with a previous report that actin synthesis is decreased by 90% in 3T3-F442A preadipocytes undergoing adipocyte differentiation [8]. In addition, the protein and mRNA expressions levels of several key ABPs, including FMN-2, GSN, and Tm-1, were changed during adipogenic induction (Fig. 2B–D). The protein levels of FMN-2 (Mr 190 kDa) and GSN (Mr 90 kDa) were decreased by 85% and 97%, respectively,

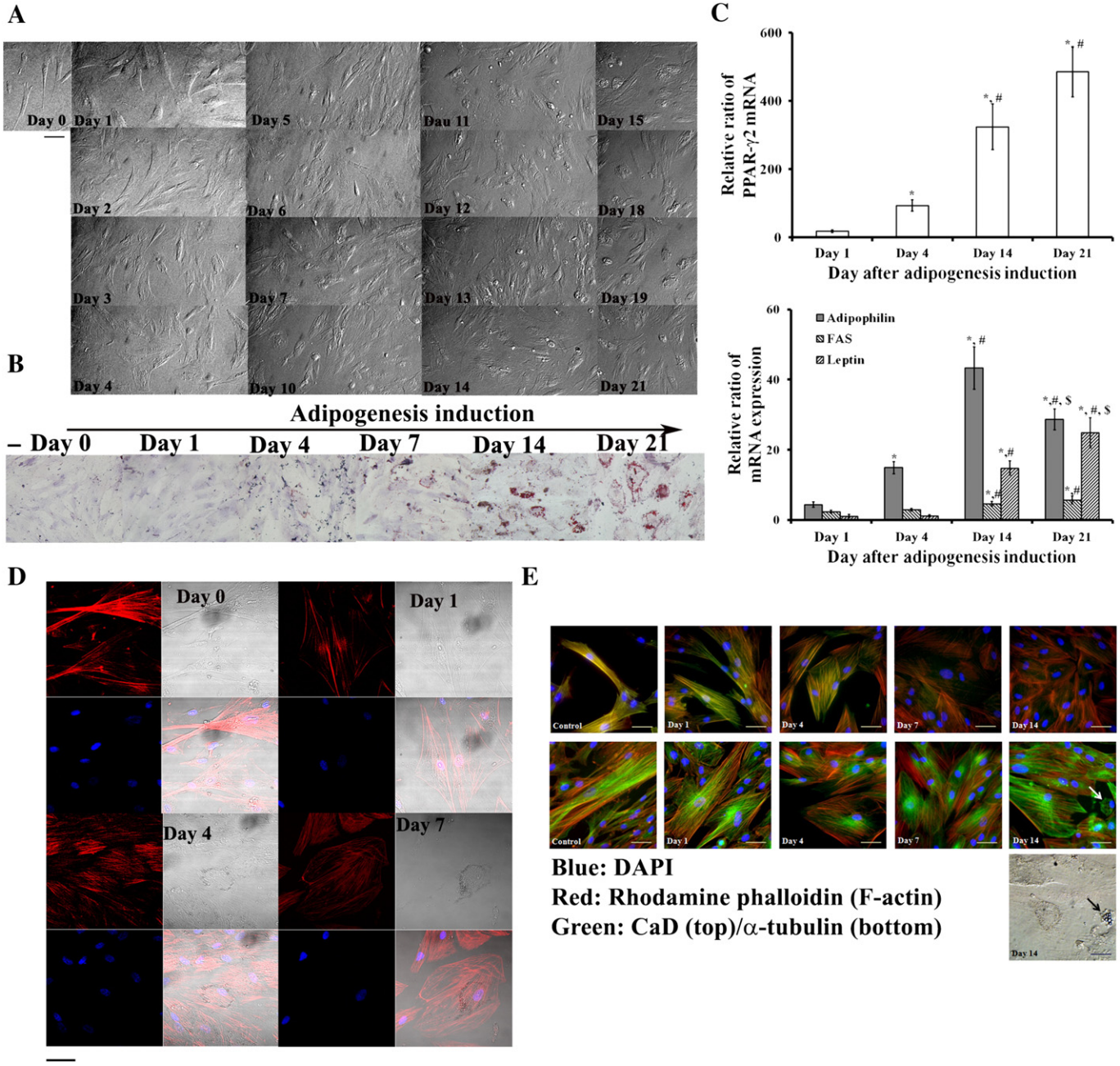
A
Day 0
Day 1
Day 5
Dau 11
Day 15
Day 2
Day 6
Day 12
Day 18
Day 3
Day 7
Day 13
Day 19
Day 4
Day 10
Day 14
Day 21
B
Adipogenesis induction
– Day 0
Day 1
Day 4
Day 7
Day 14
Day 21
C
Relative ratio of PPAR-γ2 mRNA
600
400
200
0
Day 1
Day 4
Day 14
Day 21
Day after adipogenesis induction
Relative ratio of mRNA expression
Adipophilin
FAS
Leptin
60
40
20
0
Day after adipogenesis induction
D
Day 0
Day 1
Day 4
Day 7
E
Control
Day 1
Day 4
Day 7
Day 14
Blue: DAPI
Red: Rhodamine phalloidin (F-actin)
Green: CaD (top)/α-tubulin (bottom)

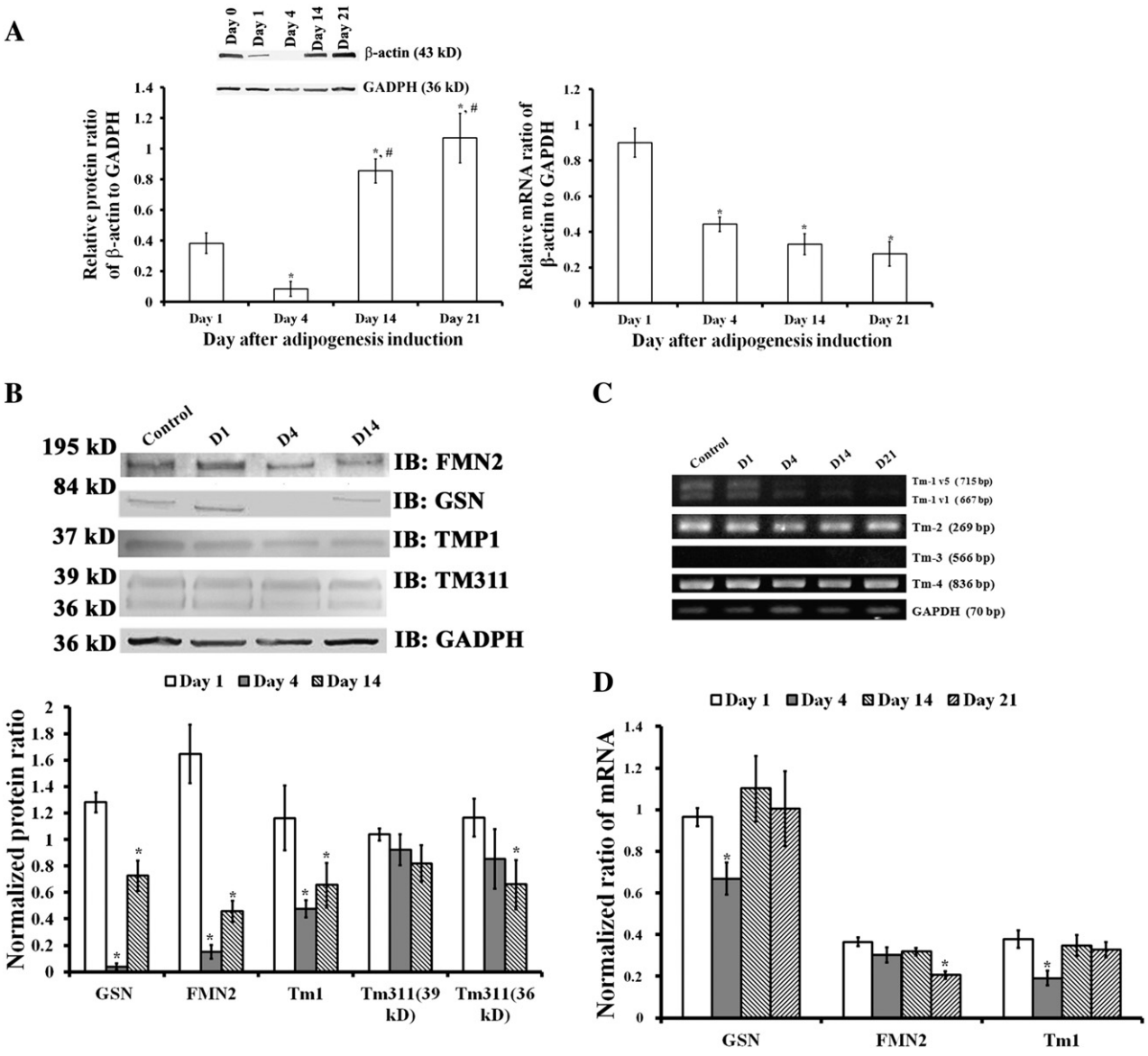


**Fig. 2.** Changes of protein level and mRNA expression for β-actin, FMN-2, GSN, and Tm1 in WJCs induced to differentiate into adipocytes. (A) (Left) Western blotting with quantitative analyses of β-actin levels in WJCs before (day 0) and after adipogenic induction for 1, 4, 14, or 21 days. GADPH was used as the loading control for data analyses. (Right) Real-time quantitative PCR (qPCR) showing changes in β-actin mRNA expression in WJCs after induction for 1, 4, 14, or 21 days. (B) Western blotting with quantitative analyses of FMN-2, GSN, and Tm levels in WJCs before (day 0) and after adipogenic induction for 1, 4, or 14 days. Using the pan-antibody TM311, two different bands at 39 kDa and 36 kDa were detected, while using the TMP1 antibody specific to Tm-1 revealed only one band at 37 kDa. (C) Agarose gels showing GADPH, Tm-1, Tm-2, Tm-3, and Tm-4 mRNA in WJCs before (day 0) and after adipogenic induction for 1, 4, or 14 days. (D) Real-time qPCR data analyses of GSN, FMN-2, and Tm1 mRNA in WJCs after induction for 1, 4, 14, or 21 days. In (A), (B), and (D), each value represents the mean ± SEM ($n = 12$). * and #, significant difference ($P < 0.05$) compared to WJCs 1 day and 4 days post-induction, respectively.

after induction for 4 days and decreased by 50% and 30%, respectively, after the subsequent induction for 14 days (Fig. 2B). Immunoblotting for all Tm isoforms in cell extracts using the antibody TM311 showed two distinct bands at 39 kDa and 36 kDa, while using the Tm-1-specific antibody TMP1 only revealed one band at 37 kDa (Fig. 2B). Using the pan-antibody TM311 revealed that the induction of adipogenic differentiation did not affect the protein levels of Tm (Fig. 2B). However, when the TMP1 antibody was used, we observed that the protein level of Tm-1 was decreased by 53% or 35% in cells after induction for 4 or 14 days, respectively (Fig. 2B).

Three isoforms, Tm-1, -2, and -4, exist in human WJCs (Fig. 2C). For Tm-1, two variants of mRNA were found with different length: a longer Tm-1 v5 and a shorter Tm-1 v1. Quantitation using real-time qPCR revealed that after induction for 4 days, there was no change

**Fig. 1.** Phenotypic transformation of WJCs differentiation into adipocytes. (A) Phase contrast microscopy showing morphological changes of WJCs during the 3 weeks of adipogenic induction. The calibration bar is 100 μm. (B) Oil red O staining showed cytoplasmic lipid droplet accumulations in WJCs during the 3 weeks of adipogenic induction. The calibration bar is 50 μm. (C) Adipogenesis was confirmed by the gene expression of PPAR-γ2, adipophilin, FAS, and leptin. Each value represents the mean ± SEM ($n = 12$). *#$, significant difference ($P < 0.05$) compared to WJCs 1 day and 4 and 14 days post-induction, respectively. (D) Confocal fluorescence microscopy visualising the rhodamine phalloidin (RP)-labelled F-actin (Red) in WJCs before (day 0) and after adipogenic induction for 1, 4, or 7 days. The nucleus was labelled with DAPI (blue). Phase contrast micrograph showing lipid droplets appeared at day 4 and 7. The calibration bar is 50 μm. (E) Colocalising CaD or α-tubulin immunofluorescence labelled (green) and RP-labelled F-actin (Red) in WJCs before (control) and after adipogenic induction for 1, 4, 7, or 14 days. The nucleus was labelled with DAPI (blue). Phase contrast micrograph (right bottom corner) showing lipid droplets associated with microtubule cytoskeleton in WJCs 14 days post-induction. The calibration bar is 50 μm. (For interpretation of the references to colour in this figure legend, the reader is referred to the web version of this article.)

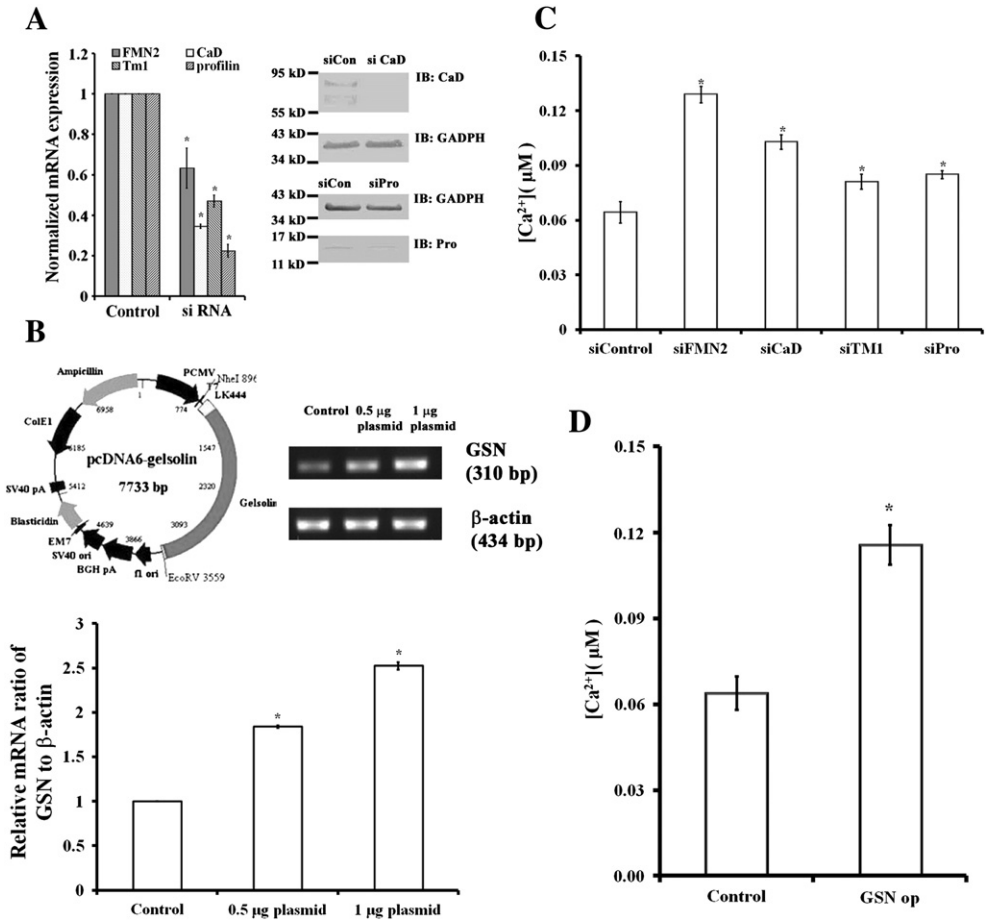


**Fig. 3.** Effects of siFMN-2, siTm-1, siCaD, siPro, and GSN op on intracellular $Ca^{2+}$ in WJCs. (A) Left: Measurements with real-time qPCR showing gene knockdown for FMN-2, Tm-1, CaD, and Pro in WJCs. Right: Immunoblotting analyses showing significantly decreased protein levels in siCaD and siPro transformed cells. (B) GSN overexpression in WJCs transfected with 0.5 or 1 μg of the pcDNA6-GSN construct. (C) Measurements of cellular $Ca^{2+}$ levels with the fura-2 fluorescence ratio (F340/F380) in siFMN-2, siTm-1, siCaD, siPro, and (D) GSN op WJCs. The values represent the mean ± SEM (n = 9), with * indicating a significant difference compared to siControl in (C) and to the control WJCs without GSN transfection in (D).

in the FMN-2 mRNA expression in the WJCs, but the expression of GSN and Tm-1 mRNA was decreased by 30% and 50%, respectively. Notably, induction for 14 or 21 days caused no significant change in the expression of FMN-2, GSN, and Tm-1 in cells (Fig. 2D). These results suggested that the downregulation of actin and ABPs (e.g., GSN, FMN-2, and Tm-1) during early adipogenic induction might be essential for the consequent commitment of WJCs to terminal adipogenic differentiation.

### 3.3. Effects of siFMN-2, siTm-1, siCaD, siPro, and GSN op on intracellular $Ca^{2+}$ in WJCs

To verify that the initial downregulation of ABPs is essential for the adipogenic differentiation process, gene knockdown by small interfering RNAs (siRNAs) specific against FMN-2 (siFMN-2), Tm-1 (siTm-1), CaD (siCaD), and Pro (siPro), as well as GSN overexpression (GSN op) were conducted in WJCs. Measurements with real-time qPCR showed 37%, 64%, 53%, and 78% knockdown for FMN-2, Tm-1, CaD, and Pro gene expression in WJCs, respectively (Fig. 3A, left panel). The immunoblot analyses revealed an almost complete loss of CaD or Pro protein in transformed WJCs (Fig. 3A, right panel). Consistent with our recent report [18], intracellular $Ca^{2+}$ was increased in transformed WJCs with siRNA-mediated silencing of FMN-2, or Tm-1, or CaD, or Pro expression (Fig. 3C). In contrast, WJCs subjected to transfection with 0.5–1 μg pcDNA6-GSN constructs (Fig. 3B, top panel) caused 1.8–2.5 folds increases in the expression ratio of GSN mRNA relative to β-actin mRNA (Fig. 3B, bottom panel) in cells. Similarly, the cellular $Ca^{2+}$ was also found to increase in GSN op WJCs (Fig. 3D). Consistent with the notion that the actin cytoskeleton could modulate intracellular $Ca^{2+}$ release in cells [30], our results showed that the destruction of F-actin filament through the downregulation of FMN-2, Tm-1, CaD, and Pro for stabilising F-actin or the upregulation of GSN for severing actin filament could positively modulate intracellular $Ca^{2+}$ signalling in WJCs.

### 3.4. Effects of siFMN-2, siTm-1, siCaD, siPro, and GSN op on the adipogenic differentiation of WJCs

A previous study using cytochalasin D to disrupt stress fibres showed that the adipogenic induction potential was enhanced in mouse embryonic stem cells [11]. In this study, siFMN-2, siTm-1, siCaD, siPro, and GSN op were used to establish the role of these ABPs in the modulation of F-actin formation in association with stress fibres that control the commitment of WJCs to adipogenic differentiation (Figs. 4 and 5). Real-time qPCR analyses showed that gene silencing of siFMN-2, siCaD, siPro, and siTm1 in WJCs promoted the expression of PPAR-γ2 (Fig. 4A, top panel), adipophilin (Fig. 4A, upper middle panel), FAS (Fig. 4A, lower middle panel), and leptin (Fig. 4A, bottom panel) at 4 or 14 days post-induction. Conversely, the mRNA expression in GSN op WJCs was decreased by 15% and 20% for PPAR-γ2 (Fig. 4B, top panel), 73% and 39% for adipophilin (Fig. 4B, upper middle panel), and 40% and 30% for FAS (Fig. 4B, lower middle panel) after induction for 4 and 14 days, respectively. However, leptin

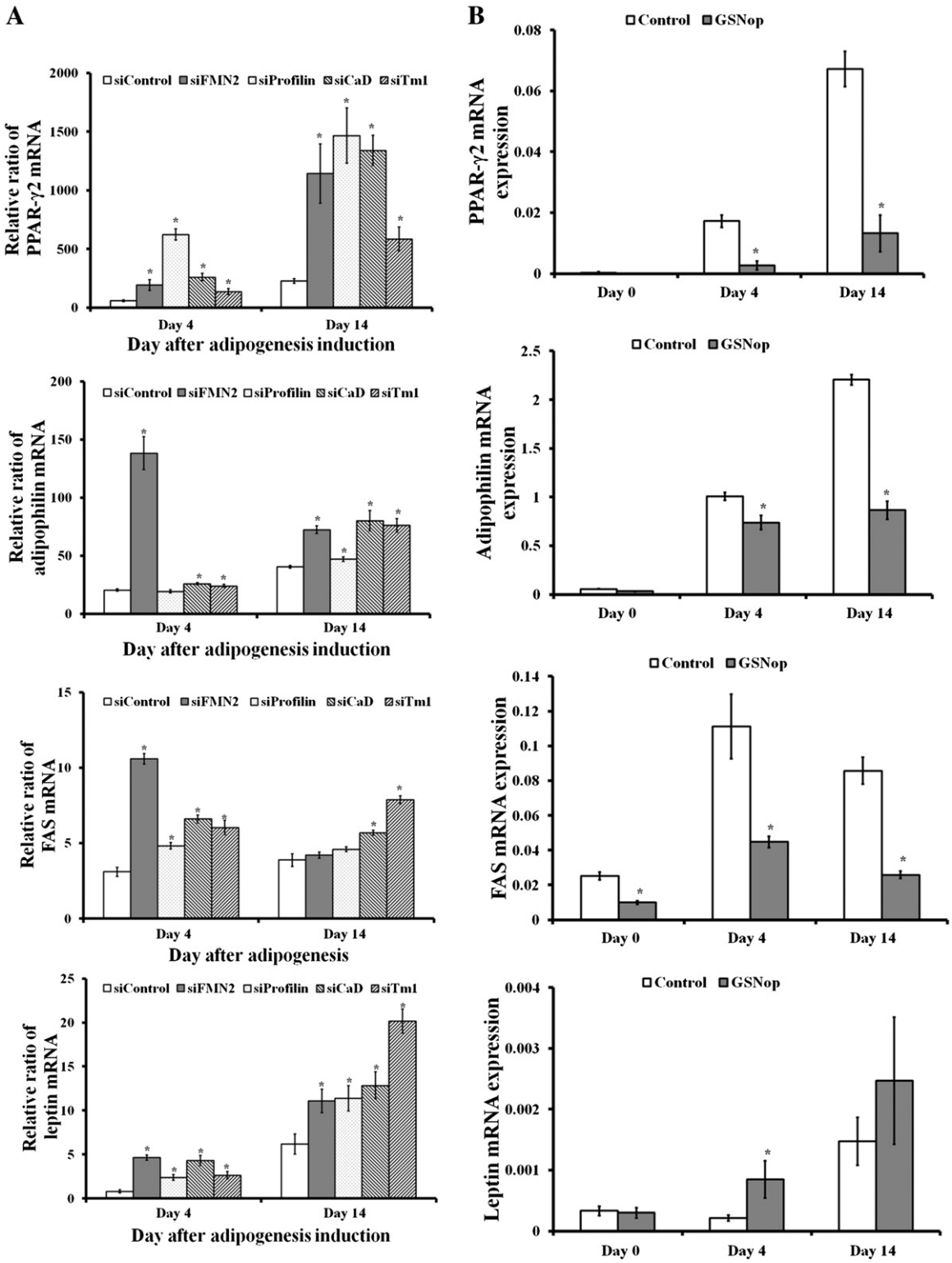


**Fig. 4.** Effects of siFMN-2, siPro, siCaD, siTm-1, and GSN op on adipocyte-related mRNA expression. (A) Gene silencing of siFMN-2, siPro, siCaD, and siTm-1 in WJCs promoted the expression of PPAR-γ2, adipophilin, FAS, and leptin in 4 or 14 days post-induction cells. (B) GSN overexpression of adipocyte-related mRNA expression, PPAR-γ2, adipophilin, FAS, and leptin in WJCs before (day 0) or after adipogenic induction for 4 or 14 days. Each value represents the mean ± SEM ($n = 9$). *, significant difference ($P < 0.05$) compared to siControl cells in (A) and compared to the control WJCs without GSN transfection in (B).

mRNA expression was increased or not significantly changed in GSN op WJCs after 4 or 14 days post-induction, respectively, as compared with the siControl cells (Fig. 4B, bottom panel).

Oil red O staining showed alterations in the potency of the commitment of siCaD, siFMN-2, and GSN op WJCs to adipogenic differentiation (Fig. 5); the lipid droplet synthesis was increased in siCaD and siFMN-2 WJCs (Fig. 5A,B) but decreased in GSN op WJCs (Fig. 5C) during adipocyte-induction. As compared with the siControls, the number and size of the lipid droplets were increased to 2.1 and 1.2 in the siFMN-2 WJCs, respectively, and to 9.0 and 1.3 in the siCaD WJCs, respectively, after adipogenic induction for 14 days (Fig. 5B). In contrast, the GSN-op WJCs retained the potential for adipogenic

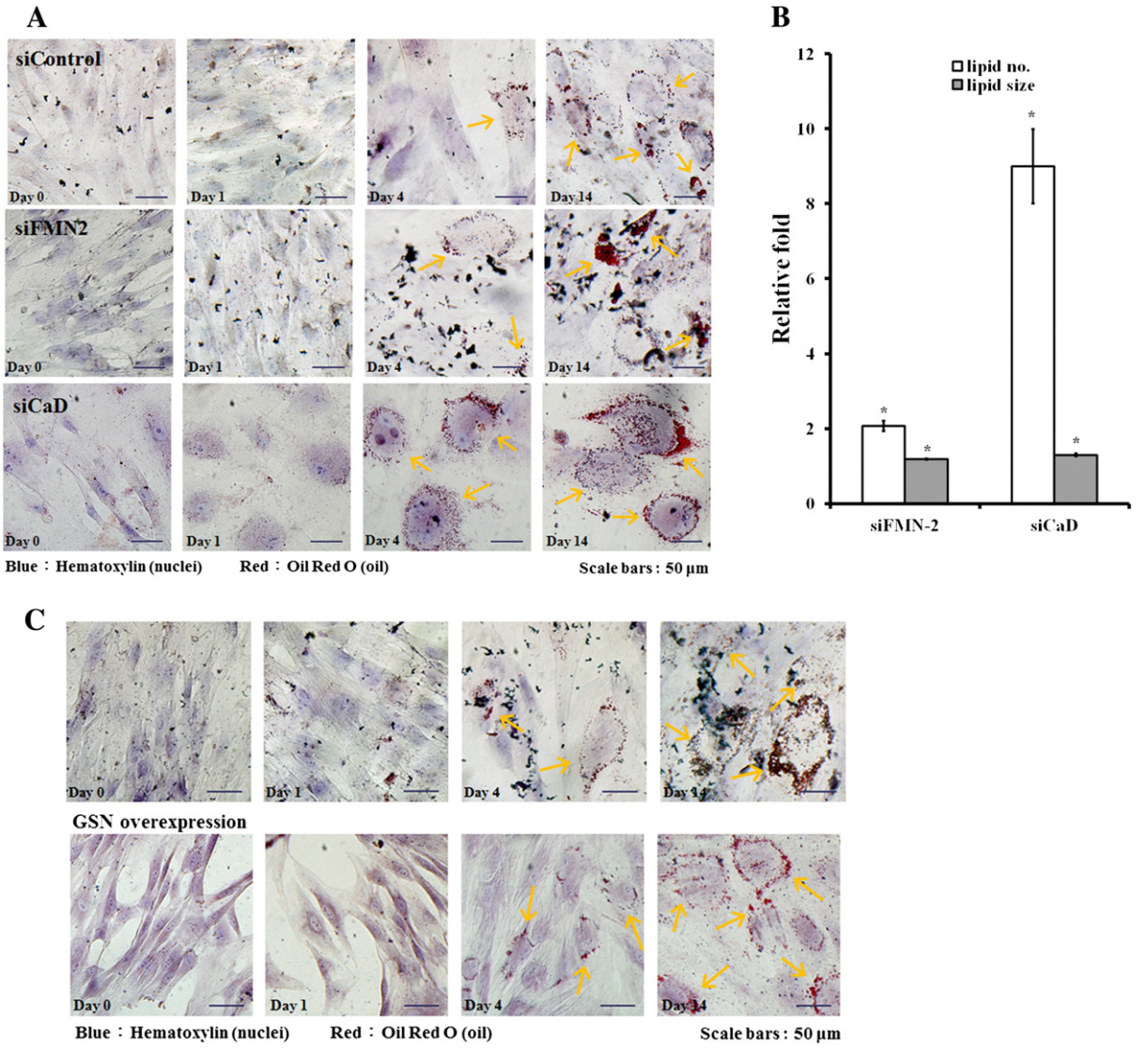


**Fig. 5.** Effects of siFMN-2, siCaD, and GSN op on the adipogenic differentiation potential of WJCs. (A) Oil red O staining showing alterations in adipogenic potency for siFMN-2 and siCaD gene-silenced WJCs commitments to adipocytes. The calibration bar is 50 μm. (B) Quantitative analyses of the lipid droplet synthesis for siFMN-2 and siCaD WJCs during adipocyte-induction. Based on the images obtained in (A), the lipid droplets number and size in cells after induction for 14 days were analysed using the computerised Image-Pro Plus software. In comparison with siControls, the values for siFMN-2 and siCaD WJCs were expressed as relative folds in increase. Three different sets of experiments with 10 images were analysed. Each value represents the mean ± SEM. *, significant difference ($P<0.05$) compared to siControl cells. (C) Oil red O staining revealed that the lipid droplet synthesis in GSN-transfected WJCs was attenuated as compared with control cells without GSN transfection. The calibration bar is 50 μm.

differentiation although the lipid droplet synthesis was decreased in GSN op WJCs as compared with controls upon adipocyte-induction (Fig. 5C). Together, these results indicated that disrupting the formation of F-actin by gene knockdown of FMN-2, Tm-1, CaD, and Pro could promote the potency of the adipogenic differentiation of WJCs, but increasing the fragmentation of F-actin by GSN overexpression in WJCs could reduce adipogenic gene expression and adipogenic potency. Apparently, cytoskeletal disassembly may not be a final determinant for promoting adipogenesis in WJC induction.

It has been shown that cytoskeletal disassembly and cell rounding could promote adipogenesis in mouse embryonic stem cells [11]. Using fluorescence microscopy to visualise the distribution of RP-labelled F-actin in cells, we observed that WJCs transfected with siCaD for 1 or 2 days (Fig. 6A, top panel) had a conspicuous cell shape change from a fibroblast phenotype to a "broader" shape. In contrast, the GSN op WJCs that were cultured for 1 or 2 days as control cells without overexpressing GSN still retained a fibroblastic cell shape (Fig. 6A, bottom panel). Laser scanning confocal microscopy also revealed that transformed cells with siRNA against FMN-2, Tm-1, and CaD for two days had a cell shape change from a spreading to a widening shape, while GSN op cells retained a fibroblast phenotype (Fig. 6B). Fig. 6C showed the morphological differences under a microscope with (Fig. 6C, bottom panel) or without (Fig. 6C, upper panel) oil red O staining for siFMN-2 and GSN op WJCs without adipogenic induction. The fibroblastic cell shape GSN op WJCs were observed to spread with less cell–cell contact, while siFMN-2 WJCs became to attach together. Clearly, both phenotypic changes of cell shape and expression level of transcription factor, PPAR-γ2 may account for the differential adipogenic potency between siRNA silencing WJCs (against FMN-2, Tm-1, CaD) and GSN-op WJCs.

### *3.5. Effects of siCaD, siPro, and GSN op on biomechanical properties of WJCs*

It has been suggested that a dynamic interplay between the cytoskeletal networks and the cell morphology plays a role in controlling mechanical properties during the adipogenic differentiation of MSCs

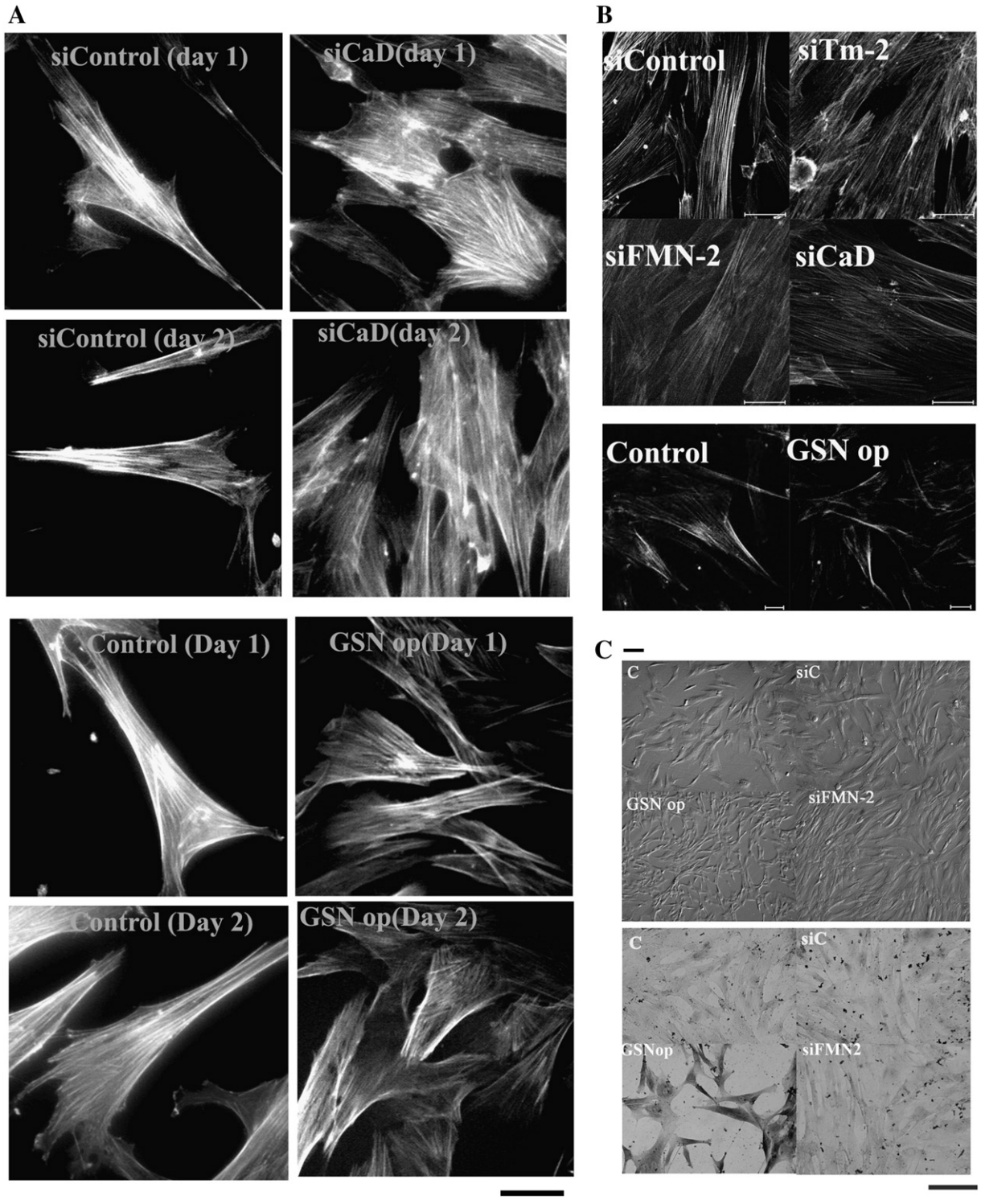


**Fig. 6.** Effects of siFMN-2, siPro, siCaD, siTm-1, and GSN op on phenotypic changes of cell shape in WJCs. (A) Fluorescence microscopy resolving RP labelled F-actin in cells revealed that siCaD transformed cells cultured for 1 or 2 days experienced conspicuous cell shape changes from a fibroblast phenotype to a "broader" shape (top panels) but no change in cell shape for GSN-transfected WJCs that were cultured for 1 or 2 days as control cells without overexpressing GSN (bottom panels). (B) Laser scanning confocal microscopy showing transformed cells with siRNA against FMN-2, Tm-1, CaD for two days had a cell shape change from a spreading to a widening shape (top panels), while GSN op cells retained a fibroblast phenotype (bottom panels). (C) The morphological differences under a microscope with (bottom) or without (upper) oil red O staining for siFMN-2 and GSNop WJCs without adipogenic induction. The calibration bar indicated in (A) (B) and (C) is 50 μm.

[11–13]. To examine the effects of inhibition of F-actin polymerisation on changes in the biomechanical characteristics of the membrane cytoskeleton in siCaD and siPro WJCs, atomic force microscopy (AFM) was performed to obtain cell surface contour images in contact mode (Fig. 7A) and to measure the interfacial forces in tapping mode (Fig. 7B–D). The V-shaped silicon cantilevers with a spring constant of ~0.9–0.12 N/m were used for imaging the cell surface areas (20×20 μm) on siControl, and siCaD, and siPro WJCs in phosphate buffer. Approximately 10–20 spots in this scanning region were randomly selected using the same probe to extend forward 1 nm deep and to retract back to the starting point (Fig. 7B). The retracting force–distance curves were used to calculate the adhesion

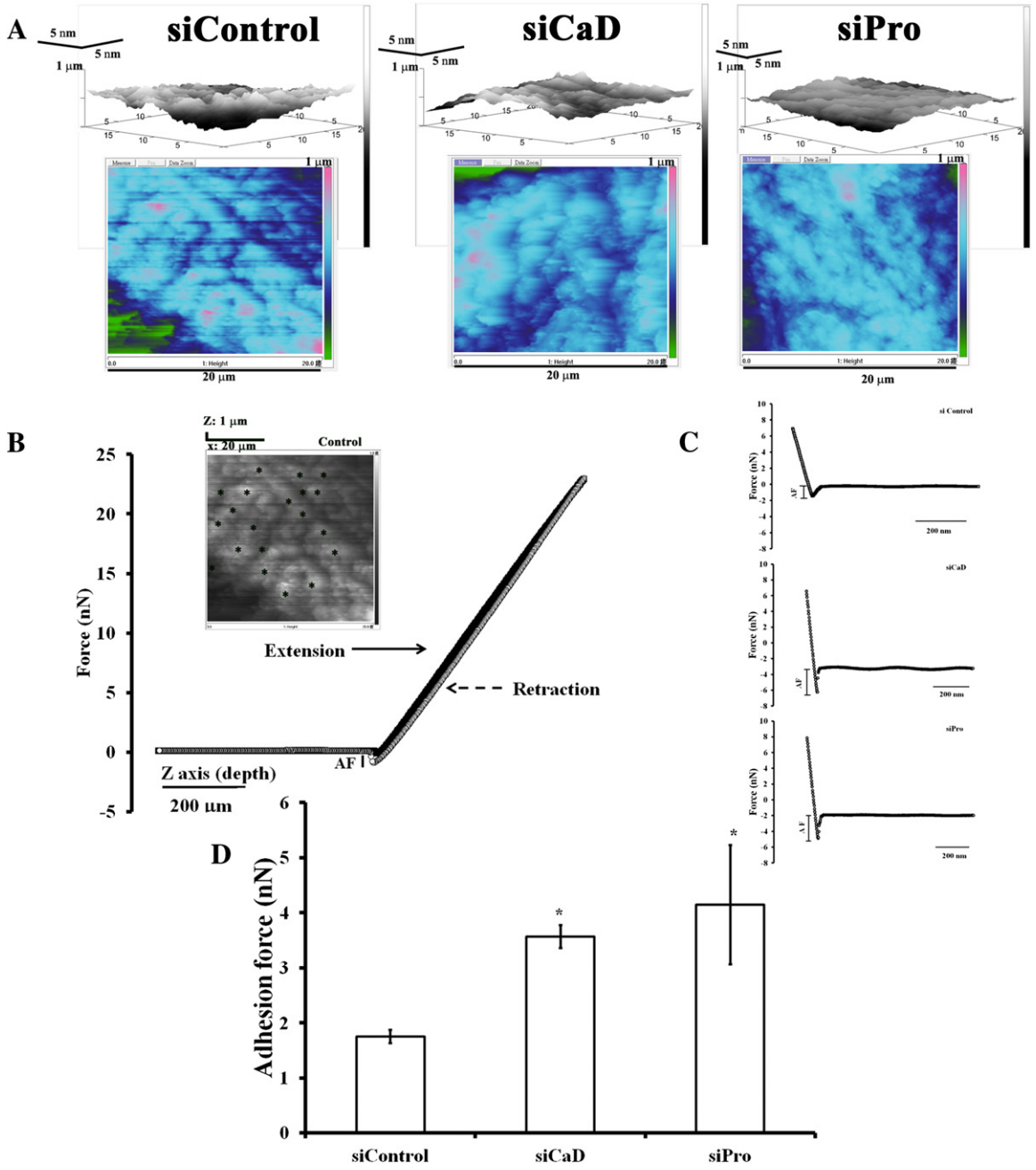


**Fig. 7.** Effects of preventing F-actin polymerisation by siCaD and siPro on changes in biomechanical characteristics of membrane cytoskeleton in WJCs. (A) Atomic force microscopy (AFM) showing the cell surface contour images and (B) the interfacial force measurements for siControl and siCaD and siPro WJCs. The V-shaped silicon cantilevers with a spring constant of ~0.9–0.12 N/m were used for imaging cell surface areas (20 × 20 μm) in siControl and siCaD WJCs in phosphate buffer. Approximately 10–20 spots in the scanning region were randomly selected using the same probe to extend forward 1 nm deep and to retract back to the starting point. (C) The retracting force-distance curves for siControl and siCaD and siPro WJCs. (D) Quantitative analysis of the adhesion force measured on cell surface for siControl and siCaD and siPro WJCs. Each value represents the mean ± SEM (n = 40, from three different cells). *, significant difference ($P<0.05$) compared to siControl cells.

forces that correspond to the elasticity of cell membrane surface (Fig. 7C). The adhesion force was 1.8 ± 0.1 and 3.6 ± 0.2 and 4.2 ± 1.0 nN for the siControl and siCaD and siPro WJCs, respectively (the average of 40 measurements from three different cells for each) (Fig. 4D). These results clearly demonstrate that the disruption of actin filament polymerisation by siCaD and siPro in WJCs caused alterations in the biomechanical signals for increasing cell adhesion forces.

The effects of F-actin fragmentation by GSN overexpression on changes in the biomechanical signals in WJCs were determined using AFM to obtain cell surface contour images (Fig. 8A) and to measure the interfacial forces in the control and GSN op WJCs in phosphate buffer (Fig. 8B,C). The adhesion force measured on the cell surface was 1.28 ± 0.1 and 2.12 ± 0.1 nN for the control and GSN op WJCs, respectively (Fig. 8C). Evidently, the upregulation of actin filament severing protein (i.e., GSN) could alter the biomechanical characteristics of the membrane cytoskeleton and modulate the adipogenic differentiation potency of WJCs.

## 4. Discussion

A previous study showed that the early occurrence of decreased cytoskeletal-protein synthesis might result in subsequent biosynthetic events specific to adipocyte differentiation via alterations in the

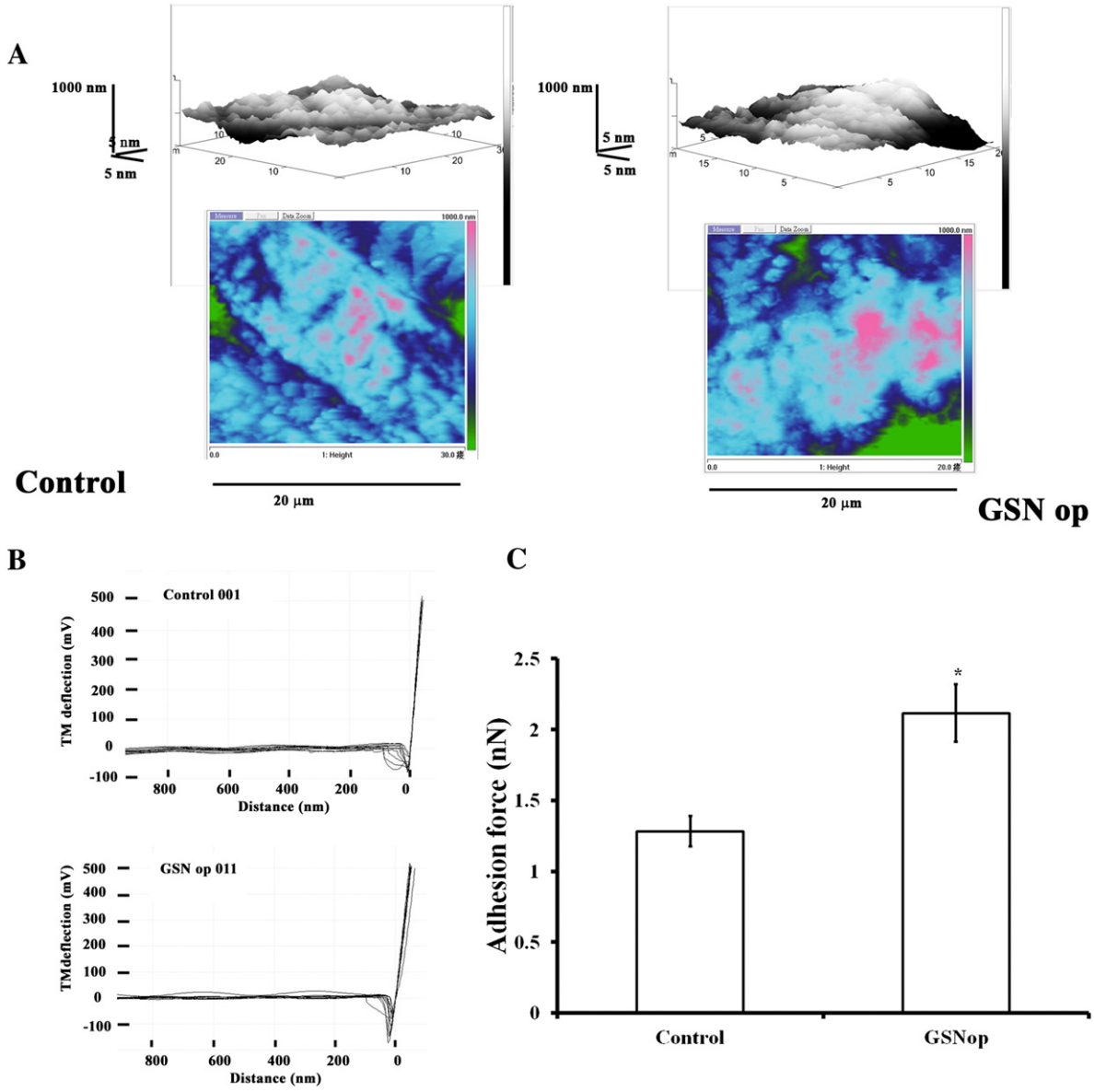


**Fig. 8.** Effects of GSN op on changes of biomechanical signals in WJCs. (A) Atomic force microscopy (AFM) showing the cell surface contour images and (B) the interfacial force measurements for control and GSN op WJCs. (C) Quantitative analysis of the cell-surface adhesion force for control and GSN op WJCs. Each value represents the mean ± SEM (n = 40, from three different cells), with * indicating significant difference ($P<0.05$) compared to the control WJCs.

cytoskeleton [8]. Analysing the adipogenic potency of human umbilical cord stromal cells (HUCSCs), Karahuseyinoglu et al. [14] revealed that adipocyte-specific markers are elevated around day 7 and level off after days 14 or 21. Based on the structural and functional data, the authors proposed that HUCSCs possess the biochemical and cellular machinery to successfully differentiate into maturing adipocytes under adipogenic conditions. In the present study, we showed that CD105-positive WJCs isolated from the human umbilical cords succeeded at differentiation into pre-adipocytes at 4 or 7 days post-induction and into adipocytes 14 or 21 days post-induction (Fig. 1). Concomitant with the phenotypic changes, the downregulation of β-actin and several key ABPs, including GSN, FMN-2, and Tm-1, in adipogenically induced WJCs was shown to occur in the early stages of adipogenic differentiation into preadipocytes (Fig. 2). Gene silencing using siRNAs against FMN-2, Tm-1, CaD, and Pro enhanced the adipogenic potency for lipid droplet accumulation and/or upregulated PPAR-γ2, adipophilin, FAS, and leptin mRNA in WJCs at 4 or 14 days post-induction (Figs. 3–5). In addition, GSN overexpression in WJCs increased intracellular $Ca^{2+}$ (Fig. 3) and cell-surface adhesion force (Fig. 8), modifying lipid droplet synthesis and downregulating the adipogenic-related gene expression of PPAR-γ2, adipophilin, and FAS, but not leptin (Figs. 4 and 5). Here, the data suggested that the temporal control of the downregulation of both actin and ABPs (e.g., GSN, FMN-2, Tm-1, CaD, and Pro) in the early stages of WJCs differentiation (Fig. 2) might act to modulate adipogenic differentiation via differential biomechanical signalling of gene expression of key regulators for adipogenesis.

Biomechanical signals, such as cell shape and spreading, play an important role in controlling stem cell commitment [11–13]. In general, plated cells have F-actin filament decorated stress fibres that are attached to the substrate, while round cells typically have cellular actin cortices underneath the membrane [31]. In addition, different cell shapes might be caused by varied interactions between actin filaments and myosin motors and might account for the

different interfacial force exerted on the different cell shapes [12]. In this study, WJCs that were subjected to adipocyte induction developed the striking cell morphological change concomitant with alterations in actin filament formation (Fig. 1). The gene silencing of FMN-2, Tm-1, CaD, and Pro produced different effects on cell shape changes and adipogenic-induction potentials in siFMN-2, siTm-1, siCaD, siPro and GSN op WJCs (Figs. 4–6). A spherical morphology was found in siFMN-2 and siTm-1 and siCaD WJCs, and a fibroblastic shape was observed in GSN op cells (Fig. 6). Round cells and cells in suspension typically have a cortical shell of F-actin fibres, while plated cells have a variably stressed network of F-actin fibres that are attached to the substrate [12]. The AFM force-distance measurements showed that disrupting actin filament polymerisation by siCaD and siPro caused a greater increase in cell adhesion force in the cells (2-fold increase, Fig. 7D) than F-actin filament severing by GSN op WJCs (65% increase, Fig. 8C). This difference in cell adhesion force might be attributed to the different phenotypic changes in cell shape. Thus, differential control of actin cytoskeleton by preventing actin filament polymerisation and facilitating actin filament severing might act differently to modulate cell shape changes in response to adipogenic induction, hence influencing WJCs commitment to adipocytes.

Kawaki et al. [32] used siGSN knockdown 3T3-L1 cells and showed that GSN silencing almost completely inhibited adipocyte differentiation. They suggested that GSN plays a crucial role in the differentiation of 3T3-L1 cells into adipocytes [33]. In the present study, GSN op WJCs retained the potential to be induced into adipocytes although the lipid droplet synthesis (Fig. 5C) and adipogenic gene expression of PPAR-γ2 (Fig. 4B, top panel), adipophilin (Fig. 4B, upper middle panel), and FAS (Fig. 4B, lower middle panel) was decreased for GSN op WJCs as compared with controls upon adipocyte induction. However, leptin mRNA expression was increased or not significantly changed in GSN op WJCs after 4 or 14 days post-induction, respectively, as compared with the siControl cells (Fig. 4B, lower panel). This finding confirmed the result obtained by oil red O staining assay that GSN-op WJCs retained the potential for induction of differentiation into adipocytes (Fig. 5C). Together, these data might suggest that GSN overexpression in WJCs could mediate PPAR-γ2-independent signalling for adipogenic induction, as reported by a recent study showing that the adipogenesis induced by pioglitazone and dexamethasone in D1 bone marrow stromal cell line might occur via a PPAR-γ and glucocorticoid receptor independent-pathway [34]. It has been shown that increasing cytoplasmic $Ca^{2+}$ inhibits adipogenesis in embryonic stem cells or 3T3-L1 preadipocytes [35]. Consistently, increasing intracellular $Ca^{2+}$ in GSN op WJCs was found to attenuate adipogenic potency (Fig. 3D). In summary, the gene expression of ABPs, which regulate the dynamics of actin filament, will affect the capability of adipogenesis in WJCs. Alterations in cell structure profoundly influence signalling events and gene expression programmes that impact the commitment of WJCs to adipogenic differentiation.

## Acknowledgements

This work was supported by the National Science Council of Taiwan government (to Y-ML., Grants: NSC-98-2320-B-005-005-MY2; NSC-100-2320-B005-001).

## Appendix A. Supplementary data

Supplementary data to this article can be found online at doi:10.1016/j.bbagen.2012.01.014.

## References

[1] M. Secco, E. Zucconi, N.M. Vieira, L.L. Fogaça, A. Cerqueira, M.D. Carvalho, T. Jazedje, O.K. Okamoto, A.R. Muotri, M. Zatz, Multipotent stem cells from umbilical cord: cord is richer than blood, Stem Cells 26 (2008) 146–150.
[2] D.L. Troyer, M.L. Weiss, Wharton's jelly-derived cells are a primitive stromal cell population, Stem Cells 26 (2008) 591–599.
[3] A. Can, S. Karahuseyinoglu, Human umbilical cord stroma with regard to the source of fetus-derived stem cells, Stem Cells 25 (2007) 2886–2895.
[4] Y.S. Fu, Y.C. Cheng, M.Y. Lin, H. Cheng, P.M. Chu, S.C. Chou, Y.H. Shih, M.H. Ko, M.S. Sung, Conversion of human umbilical cord mesenchymal stem cells in Wharton's jelly to dopaminergic neurons in vitro: potential therapeutic application for Parkinsonism, Stem Cells 24 (2006) 115–124.
[5] H.S. Wang, S.C. Hung, S.T. Peng, C.C. Huang, H.M. Wei, Y.J. Guo, Y.S. Fu, M.C. Lai, C.C. Chen, Mesenchymal stem cells in the Wharton's jelly of the human umbilical cord, Stem Cells 22 (2004) 1330–1337.
[6] C. De Bruyn, M. Najar, G. Raicevic, N. Meuleman, K. Pieters, B. Stamatopoulos, A. Delforge, D. Bron, L. Lagneaux, A rapid, simple, and reproducible method for the isolation of mesenchymal stromal cells from Wharton's jelly without enzymatic treatment, Stem Cells Dev. 20 (2011) 547–557.
[7] E.D. Rosen, C.J. Walkey, P. Puigserver, B.M. Spiegelman, Transcriptional regulation of adipogenesis, Genes Dev. 14 (2000) 1293–1307.
[8] B.M. Spiegelman, S.R. Farmer, Decreases in tubulin and actin gene expression prior to morphological differentiation of 3T3 adipocytes, Cell 29 (1982) 53–60.
[9] H.W. Heid, R. Moll, I. Schwetlick, H.-R. Rackwitz, T.W. Keenan, Adipophilin is a specific marker of lipid accumulation in diverse cell types and diseases, Cell Tissue Res. 294 (1998) 309–321.
[10] S. Klein, S.W. Coppack, V. Mohamed-Ali, M. Landt, Adipose tissue leptin production and plasma leptin kinetics in humans, Diabetes 45 (1996) 984–987.
[11] T. Feng, E. Szabo, E. Dziak, M. Opas, Cytoskeletal disassembly and cell rounding promotes adipogenesis from ES cells, Stem Cell Rev. 6 (2010) 74–85.
[12] H. Yu, C.Y. Tay, W.S. Leong, S.C. Tan, K. Liao, L.P. Tan, Mechanical behavior of human mesenchymal stem cells during adipogenic and osteogenic differentiation, Biochem. Biophys. Res. Commun. 393 (2010) 150–155.
[13] N.J. Turner, H.S. Jones, J.E. Davies, A.E. Canfield, Cyclic stretch-induced TGFbeta1/Smad signaling inhibits adipogenesis in umbilical cord progenitor cells, Biochem. Biophys. Res. Commun. 377 (2008) 1147–1151.
[14] S. Karahuseyinoglu, C. Kocaefe, D. Balci, E. Erdemli, A. Can, Functional structure of adipocytes differentiated from human umbilical cord stroma-derived stem cells, Stem Cells 26 (2008) 682–691.
[15] S. Romero, C. Le Clainche, D. Didry, C. Egile, D. Pantaloni, M.F. Carlier, Formin is a processive motor that requires profilin to accelerate actin assembly and associated ATP hydrolysis, Cell 119 (2004) 419–429.
[16] B. Leader, P. Leder, Formin-2, a novel formin homology protein of the cappuccino subfamily, is highly expressed in the developing and adult central nervous system, Mech. Dev. 93 (2000) 221–231.
[17] B. Leader, H. Lim, M.J. Carabatsos, A. Harrington, J. Ecsedy, D. Pellman, R. Maas, P. Leder, Formin-2, polyploidy, hypofertility and positioning of the meiotic spindle in mouse oocytes, Nat. Cell Biol. 4 (2002) 921–928.
[18] D.B. Shieh, R.Y. Li, J.M. Liao, G.D. Chen, Y.M. Liou, Effects of genistein on β-catenin signaling and subcellular distribution of actin-binding proteins in human umbilical CD105-positive stromal cells, J. Cell. Physiol. 223 (2010) 423–434.
[19] H.L. Yin, T.P. Stossel, Control of cytoplasmic actin gel–sol transformation by gelsolin, a calcium-dependent regulatory protein, Nature 281 (1979) 583–586.
[20] C.L. Wang, L.M. Coluccio, New insights into the regulation of the actin cytoskeleton by tropomyosin, Int. Rev. Cell Mol. Biol. 281 (2010) 91–128.
[21] C.T. Bach, S. Creed, J. Zhong, M. Mahmassani, G. Schevzov, J. Stehn, L.N. Cowell, P. Naumanen, P. Lappalainen, P.W. Gunning, G.M. O'Neill, Tropomyosin isoform expression regulates the transition of adhesions to determine cell speed and direction, Mol. Cell. Biol. 29 (2009) 1506–1514.
[22] P. Gunning, G. O'Neill, E. Hardeman, Tropomyosin-based regulation of the actin cytoskeleton in time and space, Physiol. Rev. 88 (2008) 1–35.
[23] Y.M. Liou, M. Watanabe, M. Yumoto, S. Ishiwata, Regulatory mechanism of smooth muscle contraction studied with gelsolin-treated strips of Taenia Caeci in Guinea Pig, Am. J. Physiol. Cell Physiol. 296 (2009) C1024–C1033.
[24] M.B. Humphrey, H. Herrera-Sosa, G. Gonzalez, R. Lee, J. Bryan, Cloning of cDNAs encoding human caldesmons, Gene 112 (1992) 197–204.
[25] K. Sobue, Y. Muramoto, M. Fujita, S. Kakiuchi, Purification of a calmodulin-binding protein from chicken gizzard that interacts with F-actin, Proc. Natl. Acad. Sci. U.S.A. 78 (1981) 5652–5655.
[26] R. Ishikawa, S. Yamashiro, F. Matsumura, Differential modulation of actin-severing activity of gelsolin by multiple isoforms of cultured rat cell tropomyosin. Potentiation of protective ability of tropomyosins by 83-kDa nonmuscle caldesmon, J. Biol. Chem. 264 (1989) 7490–7497.
[27] C.M. Hai, Caldesmon as a therapeutic target for proliferative vascular diseases, Mini Rev. Med. Chem. 8 (2008) 1209–1213.
[28] M.-S. Ho, F.-J. Kuo, Y.-S. Lee, C.-M. Cheng, Atomic force microscopic observation of surface-supported human erythrocytes, Appl. Phys. Lett. 91 (2007) 02390.
[29] D.J. Kwiatkowski, R. Mehl, H.L. Yin, Genomic organization and biosynthesis of secreted and cytoplasmic forms of gelsolin, J. Cell Biol. 106 (1988) 375–384.
[30] J.T. Chun, L. Santella, Roles of the actin-binding proteins in intracellular $Ca^{2+}$ signaling, Acta Physiol (Oxf.) 195 (2009) 61–70.
[31] S. Pritchard, F. Guilak, The role of F-actin in hypo-osmotically induced cell volume change and calcium signaling in anulus fibrosus cells, Ann. Biomed. Eng. 32 (2004) 103–111.
[32] A. Kawaji, Y. Ohnaka, S. Osada, M. Nishizuka, M. Imagawa, Gelsolin, an actin regulatory protein, is required for differentiation of mouse 3T3-L1 cells into adipocytes, Biol. Pharm. Bull. 33 (2010) 773–779.

[33] I. Kratchmarova, D.E. Kalume, B. Blagoev, P.E. Scherer, A.V. Podtelejnikov, H. Molina, P.E. Bickel, J.S. Andersen, M.M. Fernandez, J. Bunkenborg, P. Roepstorff, K. Kristiansen, H.F. Lodish, M. Mann, A. Pandey, A proteomic approach for identification of secreted proteins during the differentiation of 3T3-L1 preadipocytes to adipocytes, Mol. Cell. Proteomics 1 (2002) 213–222.

[34] S.H. Hung, C.H. Yeh, H.T. Huang, P. Wu, M.L. Ho, C.H. Chen, C. Wang, D. Chao, G.J. Wang, Pioglitazone and dexamethasone induce adipogenesis in D1 bone marrow stromal cell line, but not through the peroxisome proliferator-activated receptor-γ pathway, Life Sci. 82 (2008) 561–569.

[35] E. Szabo, Y. Qiu, S. Baksh, M. Michalak, M. Opas, Calreticulin inhibits commitment to adipocyte differentiation, J. Cell Biol. 182 (2008) 103–116.